Arabidopsis thaliana CYCLIC NUCLEOTIDE-GATED CHANNEL2 mediates extracellular ATP signal transduction in root epidermis

Limin Wang, Youzheng Ning, Jian Sun, Katie Wilkins, Elsa Matthus, Rose Mcnelly, Adeeba Dark, Lourdes Rubio, Wolfgang Moeder, Keiko Yoshioka, et al.

Rapid report

Arabidopsis thaliana Cyclic Nucleotide-Gated Channel2 mediates extracellular ATP signal transduction in root epidermis.

Limin Wang[1], Youzheng Ning[1], Jian Sun[1,2], Katie A. Wilkins[1], Elsa Matthus[1], Rose E. McNelly[1], Adeeba Dark[1], Lourdes Rubio[3], Wolfgang Moeder[4], Keiko Yoshioka[4], Anne-Aliénor Véry[5], Gary Stacey[6], Nathalie Leblanc-Fournier[7], Valérie Legué[7], Bruno Moulia[7], Julia M. Davies[1,*]

[1]Department of Plant Sciences, University of Cambridge, Cambridge, CB2 3EA, United Kingdom.

[2]Institute of Integrative Plant Biology, School of Life Science, Jiangsu Normal University, Xuzhou 221116, China.

[3]Departamento de Botánica y Fisiología Vegetal, Facultad de Ciencias, Universidad de Málaga, Málaga 29071, Spain.

[4]Department of Cell & Systems Biology, University of Toronto, Toronto, Ontario, M5S 3B2, Canada.

[5]Biochimie & Physiologie Moléculaire des Plantes, UMR Université Montpellier, CNRS, INRAE, Institut Agro, Montpellier 34060, France.

[6]Divisions of Plant Science and Technology, University of Missouri, Columbia 65211, MO, USA.

[7]Université Clermont Auvergne, INRA, PIAF, F-63000 Clermont-Ferrand, France.

ORCID: Wang 0000-0003-2018-3441; Sun 0000-0002-1434-4029; Wilkins 0000-0001-6513-856X; Matthus 0000-0002-7845-3945; Rubio 0000-0002-7747-2722; Moeder 0000-0003-3889-6183; Yoshioka 0000-0002-3797-4277; Véry 0000-0003-1961-5243; Stacey 0000-0001-5914-2247; Leblanc-Fournier 0000-0002-6079-1583; Legué 0000-0001-6626-5149; Moulia 0000-0002-3099-0207; Davies 0000-0003-2630-4339.

Author for correspondence: Julia Davies, Department of Plant Sciences, University of Cambridge, Cambridge CB2 3EA, United Kingdom, 44 (0)1223 333 939, jmd32@cam.ac.uk

Received: *27 August 2021*

This article has been accepted for publication and undergone full peer review but has not been through the copyediting, typesetting, pagination and proofreading process, which may lead to differences between this version and the Version of Record. Please cite this article as doi: 10.1111/NPH.17987

Accepted: *16 January 2022*

Summary

- Damage can be signalled by extracellular ATP (eATP) using plasma membrane (PM) receptors to effect cytosolic free Ca^{2+} ($[Ca^{2+}]_{cyt}$) increase as a second messenger. The downstream PM Ca^{2+} channels remain enigmatic. Here, the *Arabidopsis thaliana* Ca^{2+} channel subunit Cyclic Nucleotide-Gated Channel2 (CNGC2) was identified as a critical component linking eATP receptors to downstream $[Ca^{2+}]_{cyt}$ signalling in roots.
- eATP-induced changes in single epidermal cell PM voltage and conductance were measured electrophysiologically, changes in root $[Ca^{2+}]_{cyt}$ were measured with aequorin and root transcriptional changes were determined by qRT-PCR. Two *cngc2* loss of function mutants were used: *cngc2-3* and *dnd1* (which expresses cytosolic aequorin).
- eATP-induced transient depolarisation of *Arabidopsis* root elongation zone epidermal PM voltage was Ca^{2+}-dependent, requiring CNGC2 but not CNGC4 (its channel co-subunit in immunity signalling). Activation of PM Ca^{2+} influx currents also required CNGC2. The eATP-induced $[Ca^{2+}]_{cyt}$ increase and transcriptional response in *cngc2* roots were significantly impaired.
- CNGC2 is required for eATP-induced epidermal Ca^{2+} influx, causing depolarisation leading to $[Ca^{2+}]_{cyt}$ increase and damage-related transcriptional response.

Keywords: *Arabidopsis*; calcium; Cyclic Nucleotide-Gated Channel2 (CNGC2); CNGC4; depolarisation; extracellular ATP; plasma membrane potential; root epidermis.

Introduction

Extracellular ATP (eATP) has been shown to contribute to plant growth and development, stress responses, immunity and damage (Matthus *et al*., 2019a). Two plasma membrane (PM) co-receptors for eATP, P2K1/DORN1 (DOes not Respond to Nucleotides1) and P2K2 have been identified recently in *Arabidopsis thaliana*, with P2K1/DORN1 trans-phosphorylating P2K2 (Choi *et al*., 2014; Pham *et al*., 2020). P2K1/DORN1 commands an eATP-dependent transient increase of cytosolic free calcium ($[Ca^{2+}]_{cyt}$) as a second messenger (Choi *et al*., 2014). The root $[Ca^{2+}]_{cyt}$ response to eATP (the "signature") has a greater reliance on Ca^{2+} influx across the PM than the release of Ca^{2+} from intracellular stores (Demidchik *et al*., 2009; Rincón-Zachary *et al*., 2010). Lowering external Ca^{2+} from 10 to 0.1 mM causes an 85% decrease in the $[Ca^{2+}]_{cyt}$ response (Demidchik *et al*., 2003). Ca^{2+} influx across the PM helps explain the depolarising effect that eATP has on root PM voltage (Lew and Dearnaley, 2000; Dindas *et al*., 2018), especially given that eATP causes instantaneous $[Ca^{2+}]_{cyt}$ increase and a cytosolic acidification consistent with PM H^+-ATPase inhibition in *Arabidopsis* roots (Waadt *et al*., 2020). Indeed, patch clamp electrophysiology has revealed eATP- and P2K1/DORN1-dependent Ca^{2+}-permeable channel conductances in *Arabidopsis* root epidermal PM (Demidchik *et al*., 2009; Wang *et al*., 2018, 2019) that could contribute to PM depolarisation and $[Ca^{2+}]_{cyt}$ increase. However, the identity of the channels remains unknown. Here, data support the involvement of a Cyclic Nucleotide Gated Channel (CNGC).

Arabidopsis has a family of twenty CNGC channel subunits with members contributing to $[Ca^{2+}]_{cyt}$ signatures evoked by abiotic stress, pathogen attack and hormones (Jarratt-Barnham *et al*., 2021). Because eATP accumulates during pathogen infection and acts as a Damage-Associated Molecular Pattern (DAMP) that drives a transcriptional response through P2K1/DORN1 (Choi *et al*., 2014; Jewell *et al*., 2019; Kumar *et al*., 2020), CNGCs involved in pathogen sensing could also be acting in the eATP pathway. CNGC2 is a key candidate for testing as it operates in root signalling (Chakraborty *et al*., 2021), it is involved in both DAMP and PAMP (Pathogen-Associated Molecular Pattern) signalling, and it generates a PM hyperpolarisation-activated Ca^{2+} permeable channel conductance (Qi *et al*., 2010; Tian *et al*., 2019). CNGC2's closest paralogue, CNGC4, can interact with CNGC2 and these two subunits are hypothesised to form a heteromeric channel in PAMP signalling (Chin *et al*., 2013; Tian *et al*., 2019). CNGC2 and CNGC4 could

potentially work together in the eATP pathway.

Here, two *Arabidopsis cngc2* loss of function mutants were used: *cngc2-3* and *dnd1* (which expresses cytosolic aequorin). eATP-induced depolarisation of PM voltage has been used as a diagnostic of PM Ca^{2+} channel activity in single epidermal and cortical root cells. Results show an absolute requirement for CNGC2 but not CNGC4 in the epidermis. Patch clamp electrophysiological analysis of eATP-induced PM Ca^{2+} influx conductance of epidermal cells confirmed an absolute requirement for CNGC2. Both root eATP-induced $[Ca^{2+}]_{cyt}$ signature and transcriptional response were impaired by loss of CNGC2 function.

Materials and Methods

Plant material

Arabidopsis lines were in the Columbia (Col-0) ecotype. *dorn1-1, dorn1-3,p2k2* and *p2k1p2k2* mutants were as described previously (Choi *et al*., 2014; Pham *et al*., 2020). *cngc2-3* (T-DNA insertion line Salk-066908) was described previously by Chin *et al*., 2013. Complemented *cngc2-3* was generated with the CNGC2 coding sequence under the control of its endogenous promoter (Methods S1). *dnd1* (*defence not death1*) *cngc2* loss of function mutant constitutively expressing cytosolic (apo)aequorin) was described by Qi *et al*., 2010. *cngc4-5* (SALK_081369; Tian *et al*., 2019) was obtained from NASC. Genotyping of insertional and complemented mutants is described in Methods S1. Primers are listed in Table S1. Growth conditions are described in Methods S2. Seven- to 14-day-old plants were used unless stated otherwise.

Membrane potential measurements

Plasma membrane potential (E_m) of root elongation zone cells was measured using a glass microelectrode. A plant was fixed in a plexiglass chamber and immersed in assay solution (10 mL) containing (in mM) 2 $CaCl_2$ (± 5 EGTA or ± 0.5 $LaCl_3$), 0.1 KCl, 1 MES/Tris (pH 6.0) for at least 30 minutes before impalement. Microelectrode construction, recording circuitry and impalement are described in Methods S3. After observing a stable E_m (> 6 minutes), eATP (MgATP or Na_2ATP; Sigma) was added to the chamber (final concentration 300 μM in the assay medium, pH 6.0). In controls, $MgSO_4$ or Na_2SO4 was added.

Patch clamp recordings

Protoplasts were isolated from root elongation zone epidermis, with origin confirmed using the N9093 epidermal-specific green fluorescent protein reporter line as described by Wang *et al*., (2019). Details of isolation, patch clamp solutions and protocols are in Methods S4.

$[Ca^{2+}]_{cyt}$ measurement

Excised primary roots of Col-0 and *dnd1* expressing cytosolic (apo)aequorin were used for luminescence-based quantification of $[Ca^{2+}]_{cyt}$. Roots were placed individually into a 96-well plate (one root per well) and incubated overnight at room temperature in darkness with 10 µM coelenterazine in 100 µL of buffer; (in mM) 2 $CaCl_2$, 0.1 KCl, 1 MES/Tris (pH 5.6). $CaCl_2$ was included to maintain a similar level to that of the growth medium. Samples were washed with coelenterazine-free buffer and left to recover for at least 20 minutes in darkness. A FLUOstar OPTIMA plate reader (BMG Labtech) was used to record luminescence as described in Matthus *et al*., 2019b. $[Ca^{2+}]_{cyt}$ was calculated as described by Knight *et al*., 1997.

Analysis of gene expression

Total RNA was extracted from roots (frozen in liquid nitrogen) using the RNAeasy Plant Mini Kit (QIAGEN) and subjected to DNase I treatment (RNAse-free DNAse kit, QIAGEN). Complementary DNA (cDNA) was synthesised using the QuantiTect Reverse Transcription Kit (QIAGEN). qRT-PCR was performed in a Rotor-Gene 3000 thermocycler with the Rotor-Gene™ SYBR® Green PCR Kit (QIAGEN). *UBQ10* and *TUB4* acted as internal controls. Primers are listed in Table S1. Further details are in Methods S5.

Statistical analysis

Data normality was first analysed with the Shapiro-Wilk test in the R programme. Student's *t*-test or Tukey's HSD was used for parametric data comparison whereas the Mann-Whitney *U* test was used to compare the non-parametric data.

Results

AtCNGC2 mediates the eATP-induced depolarisation of root epidermal PM voltage and does not require AtCNGC4

The stable resting membrane voltage (E_m) of a single Col-0 root elongation zone epidermal cell (Fig.1a) was significantly but transiently depolarised by 300 µM eATP (Fig.1b). This concentration of eATP was found previously to activate a PM Ca^{2+} influx conductance in this cell type (Wang *et al*., 2019). Mean maximal depolarisation from -118.9 ± 4.8 mV to -69.2 ± 7.6 mV (Fig.1c,d; Table S2) occurred 1.8 ± 0.3 min after eATP application (MgATP or Na_2ATP) and E_m recovered fully after 14.7 ± 2.2 minutes (Fig.1e,f) in the continued presence of eATP. In controls, neither 300 µM $MgSO_4$ nor 300 µM Na_2SO_4 (Fig. 1g,h; Fig.S1a,b) affected E_m, confirming that the response was due to eATP. Incubation with 5 mM EGTA (to chelate extracellular Ca^{2+}) abolished the response to 300 µM eATP (Fig. 1g,h; Fig. S1c), showing that depolarisation required Ca^{2+} influx. However, as EGTA treatment resulted in a less negative E_m that could have compromised depolarisation, a further test of Ca^{2+} influx was conducted. Addition of 0.1 mM $LaCl_3$ as a blocker of PM Ca^{2+}-permeable channels prevented significant depolarisation by eATP (Fig. 1g,h; Fig. S1d). The loss of function *cngc2-3* mutant (T-DNA insert in second exon) and the complemented *cngc2-3,CNGC2::CNGC2* mutant (Fig. S2a-c) were then analysed. Expression levels of *P2K1/DORN1* and the co-receptor *P2K2* were normal in *cngc2-3* roots, indicating that eATP perception itself would be unimpaired (Fig.S2d). There were no significant differences in resting E_m between genotypes (Table S2). In contrast to Col-0, 300 µM eATP failed to depolarise *cngc2-3* E_m (Fig.1b-d; Table S2). Complementation fully restored the mutant's E_m response to eATP (depolarisation and recovery time) (Fig. 1b-e), but maximum E_m depolarisation occurred sooner than Col-0 (Fig. 1f). This may reflect the approximately doubled abundance of *CNGC2* transcript in the complemented mutant, although this was not statistically significant (Fig.S2e). To verify the *cngc2-3* results, the *CNGC2 dnd1* mutant (Fig. S3a-c) was also tested. This has a single point mutation causing a stop codon in the third exon and expresses cytosolic aequorin (Qi *et al*., 2010). Resting *dnd1* E_m was not significantly different to those of other genotypes and was unaffected by eATP treatment (Fig.S3d-f, Table S2). These results show that the eATP-induced and Ca^{2+}-dependent PM E_m response is reliant on CNGC2.

Elongation zone epidermal cells of the *dorn1-3* loss of function mutant, the *dorn1-1* kinase mutant and the *p2k2* mutant all retained a small but significant depolarisation of E_m when challenged with 300 µM eATP (Fig.S4a-d, Table S2). *CNGC2* transcript levels were normal in both *dorn1-3* and *p2k2* mutant roots, so their lowered response is most likely due to loss of receptor function rather than channel function (Fig.S4e). The *dorn1-3p2k2* double mutant (*p2k1p2k2*) also sustained a

small but significant depolarisation of E_m when challenged with 300 μM eATP but this was not significantly different to that caused by the Na_2SO_4 control (Fig. S5a-c; Table S2; p = 0.74). Under control conditions, the *p2k1p2k2* mutant had a significantly more negative E_m (-143.9 ± 4.3 mV; n = 10) than its paired Col-0 wild type
(-129.9 ± 4.6 (n = 5); p = 0.005) and this may help explain why Na^+ caused a depolarisation in this mutant but not Col-0. Overall the results suggest that the two receptors working together are sufficient to initiate the eATP-induced depolarisation of E_m and that CNGC2 is an absolute requirement in this cell type.

CNGC2 has been shown to interact with CNGC4 in immune signalling (Chin *et al*., 2013; Tian *et al*., 2019). Here, the root elongation zone epidermis of the *cngc4*-5 loss of function mutant (Fig. S6a-d) was impaled and tested with 300 μM eATP. eATP caused a significant depolarisation of E_m to -69.4 ± 10.9 mV, similar to Col-0 wild type (p > 0.05; Fig. S6e-g, Table S2). These results show that CNGC2 controls the PM E_m response to eATP without the need for CNGC4.

Plasma membrane Ca^{2+} currents induced by eATP in Col-0 root epidermal protoplasts require CNGC2

Whole-cell currents across the PM of root elongation zone epidermal protoplasts (Wang *et al*. (2019) of Col-0 and *cngc2-3* were recorded. No significant differences in control currents or reversal potential were found between genotypes (mean ± SE reversal potential: Col-0 -59 ± 16.3 mV, n = 4; *cngc2-3* -35 ± 8.9, n = 4). For Col-0, 300 μM eATP activated whole-cell inward current upon membrane hyperpolarisation, but not outward current upon membrane depolarisation (Fig. 2a). No effect of Na^+ as the salt control was found in previous trials (Wang *et al*., 2018, 2019). Analysis of the reversal potential of eATP-activated currents (average control (-ATP) currents were subtracted from average eATP-activated currents (Wang *et al*., 2013) revealed an approximate value of +22 mV (n = 4), far from the equilibrium potentials of K^+ (-79 mV) and Cl^- (-28 mV) and indicating Ca^{2+} permeability. eATP-activated inward current was significantly inhibited by 100 μM Gd^{3+}, a plant Ca^{2+} channel blocker that is effective against CNGC2 (Demidchik *et al*., 2009; Tian *et al*., 2019; Wang *et al*., 2018, 2019; Fig. 2a). These results suggest that Ca^{2+} influx across the PM contributed to the eATP-activated current in Col-0. As Gd^{3+} is an effective blocker of a variety of PM Ca^{2+}-permeable channels (Demidchik *et al*., 2002, 2009;

Wang *et al*., 2018, 2019) it is likely that it also blocked Ca^{2+}-permeable channels that were *not* activated by eATP, causing the significant reduction in inward current in the presence of both eATP and Gd^{3+} to below the control value. The eATP-activated Ca^{2+} inward current was absent from *dorn1-3* PM (Fig.S7). At resting E_m of Col-0 epidermal cells (around -120 mV) the eATP-activated current would deliver Ca^{2+} to the cytosol which would both elevate $[Ca^{2+}]_{cyt}$ and initiate depolarisation. It can be inferred that some eATP-activated Ca^{2+} influx should have occurred in membrane voltage trials at the less negative E_m caused by EGTA (-85.2 ±- 5.4 mV; Fig. 1g,h, Fig.S1c) but this was not observed, further supporting the role of Ca^{2+} influx in eATP-induced depolarisation of E_m. In contrast to Col-0, PM whole-cell currents of *cngc2-3* (either inward or outward) failed to respond to 300 µM eATP (Fig. 2b). Gd^{3+} (100 µM) blocked inward and outward currents in the presence of eATP, but these currents were not investigated further (Fig.2b). Thus results strongly suggest that the eATP-activated inward current in Col-0 would be due to the hyperpolarisation-activated Ca^{2+} influx through CNGC2, helping to explain how eATP failed to depolarise the E_m of the *cngc2* mutants.

eATP-induced $[Ca^{2+}]_{cyt}$ increase in roots is impaired in *dnd1*

The requirement for CNGC2 in eATP-activated epidermal PM depolarisation and Ca^{2+} influx conductance and should manifest in impaired eATP-induced $[Ca^{2+}]_{cyt}$ elevation in the *dnd1* mutant, which expresses cytosolic (apo)aequorin as a bioluminescent $[Ca^{2+}]_{cyt}$ reporter. The typical monophasic $[Ca^{2+}]_{cyt}$ increase ("touch response") after NaCl addition (control for mechanostimulation and cation effect of Na_2ATP) was observed in individual roots of Col-0 and *dnd1*. Amplitude of the touch peak and total $[Ca^{2+}]_{cyt}$ mobilised did not differ significantly between genotypes (Fig. 3a). In contrast, 300 µM eATP caused a biphasic $[Ca^{2+}]_{cyt}$ increase (after the touch response) in both Col-0 and *dnd1* roots (Fig. 3b), confirming that this part of the $[Ca^{2+}]_{cyt}$ signature was caused by eATP. This biphasic signature ("peak 1" and "peak 2") was observed in previous studies on *Arabidopsis* roots and seedlings using aequorin (Demidchik *et al*., 2003; Tanaka *et al*., 2010; Matthus *et al*., 2019a, b; Mohammad-Sidik *et al*., 2021) and also root tips using YC3.6 (Tanaka *et al*., 2010). *dnd1* roots were significantly impaired in the amplitude of both of the eATP-induced $[Ca^{2+}]_{cyt}$ peaks and also total $[Ca^{2+}]_{cyt}$ mobilised (Fig. 3d). Significant impairment was also observed at 100 µM and 1 mM eATP (Fig.S8). Since P2K1/DORN1 governs the eATP-induced $[Ca^{2+}]_{cyt}$ signature in *Arabidopsis* roots (Matthus *et al*., 2019a), impairment of

the $[Ca^{2+}]_{cyt}$ response in *dnd1* helps place CNGC2 downstream of that eATP receptor, consistent with the electrophysiological data presented here.

Root cortical PM depolarisation does not require CNGC2 but may require CNGC4

The residual eATP-induced $[Ca^{2+}]_{cyt}$ increase seen in *dnd1* roots suggests CNGC2-independent Ca^{2+} influx pathways in other cells such as the cortex. Cortical cells also increase $[Ca^{2+}]_{cyt}$ in response to eATP (Krogman *et al*., 2020). CNGC2 redundancy was investigated by measuring elongation zone cortical cell E_m. Resting Col-0 cortical cell E_m was -131.6 ± 9.1 mV (Fig. S9a; Table S2), which was not significantly different to the epidermis. Application of eATP (300 µM) to the root transiently and significantly depolarised the cortical PM (Fig. S9a; Table S2). There was no significant difference between cortex and epidermis in terms of the maximum depolarisation amplitude, the time to reach the maximum depolarisation or recovery time. The E_m of elongation zone cortical cells in the two CNGC2 mutants was then investigated. Unlike the null response of epidermal cells of *cngc2-3* and *dnd1*, addition of eATP to the root triggered cortical E_m depolarisation in both mutants (Fig. S9b,c; Table S2). No significant difference in the PM E_m before (-ATP) or after ATP (+ATP) was observed between Col-0 and these two mutants (Fig. S9e), indicating that CNGC2 is not involved in this cell type. The *cngc4-5* mutant still supported a significant depolarisation of cortical E_m when eATP was added to the root (Fig. S9d,e; Table S2) but this was significantly smaller than that found previously in its epidermal cells (cortex, 21.6 ± 6.8 mV; epidermis, 62.2 ± 8.8 mV; $p = 0.012$). This indicates a CNGC4-dependent pathway in the cortex. The residual depolarisation in the *cngc4-5* implies involvement of other CNGCs (but not CNGC2) or other transport systems (Fig S9f). Together the results help explain the residual eATP-induced $[Ca^{2+}]_{cyt}$ increase in *dnd1* roots; CNGC2 does not operate in all other cells.

CNGC2 is implicated in eATP-responsive gene expression

The eATP-responsive transcriptome is highly enriched in defence-related and wound-response genes, including Mitogen-Activated Protein Kinase 3 (*MPK3*), WRKY DNA-Binding Protein 40 (*WRKY40*), Calcium-Dependent Protein Kinase 28 (*CPK28*) and the cysteine protease Metacaspase 7 (*MC7*) (Choi *et al*., 2014; Jewell *et al*., 2019). Transcriptional upregulation of those genes by eATP is P2K1/DORN1-dependent (Choi *et al*., 2014; Jewell *et al*., 2019) and their

response to eATP was examined here in Col-0, *cngc2-3* and *cngc2-3,CNGC2*::*CNGC2* roots by qRT-PCR. eATP (300 μM for 30 minutes) significantly up-regulated expression of all four genes in Col-0, with no significant difference between Col-0 and *cngc2-3,CNGC2*::*CNGC2* (Fig.4). However, transcript levels of *MPK3, WRKY40, CPK28* and *MC7* were all significantly lower in *cngc2-3* compared to Col-0 or (with the exceptions of *CPK28* and *MC7*) compared to *cngc2-3,CNGC2*::*CNGC2* (Fig.4). Thus, CNGC2 can be required for the eATP transcriptional response.

Discussion

Effects of eATP on plants were reported almost half a century ago (Jaffe, 1973) yet relatively few components of eATP signalling pathways have been identified. A forward genetic screen based on eATP's ability to increase $[Ca^{2+}]_{cyt}$ led to the identification of the first angiosperm eATP receptor, P2K1/DORN1 (Choi *et al*., 2014). Here, eATP's ability to depolarise root PM E_m (Lew and Dearnaley, 2000) was used in a targeted gene approach. Depolarisation can arise from Ca^{2+} influx across the PM (Dindas *et al*., 2018) and eATP causes a rapid $[Ca^{2+}]_{cyt}$ increase in roots that could initiate depolarisation (Waadt *et al*., 2020) as a multi-conductance process (Wang *et al*., 2019). Here, eATP-induced depolarisation required extracellular Ca^{2+} (Fig. 1g,h; Fig. S1c,d), showing its reliance on Ca^{2+} influx. Thus, the unresponsiveness of *cngc2* mutant root elongation zone epidermal PM to eATP (Fig. 1) is consistent with its lack of eATP-induced PM Ca^{2+} influx currents (Fig. 2) and reveals CNGC2 as a necessary component for initiating depolarisation downstream of P2K1/DORN1/P2K2 in young epidermal root cells (Fig.4e).

CNGC2 works together with CNGC4 in PAMP signalling, acting as a heterotrimeric Ca^{2+} channel in the flg22 pathway (Chin *et al*., 2013; Tian *et al.*, 2019). During the course of this study, Wu *et al*. (2021) reported that *Arabidopsis* pollen grain PM has an eATP-activated Ca^{2+} influx conductance, measured using whole-cell patch clamp electrophysiology. This conductance was impaired in both a single mutant of CNGC2 and a single mutant of CNGC4, suggesting that these two channel sub-units might work together to facilitate germination. Whether CNGC2 and CNGC4 underpin eATP-induced $[Ca^{2+}]_{cyt}$ elevation and transcription in pollen remains untested. Here, with eATP as a potential DAMP, CNGC2 could be acting either as a homotetramer or a heterotetramer (that includes CNGC4) in the root epidermis but in either event it is the obligate component of the depolarisation response given CNGC4's redundancy (Fig. S5e-g, Table S2). If a

heterotetramer included CNGC4 (which is expressed at almost half the level of CNGC2 in the epidermis; Dinneny *et al*., 2008), that CNGC4 sub-unit could be replaced. This is in contrast to CNGC4's pivotal role in the PAMP signalling CNGC2/4 heterotetramer, where CNGC4 is the phosphorylation target of the BIK1 kinase (Tian *et al*., 2019).

A residual $[Ca^{2+}]_{cyt}$ signature and transcriptional response were still observed in CNGC2 mutants, showing that other channels are involved in the root's overall response to eATP that now need to be identified. Results here from the cortex implicate a role for CNGC4 (Fig.4e; Fig.S9f). Annexin1 is implicated at whole root level but its mode of action is not yet determined (Mohammad-Sidik *et al*., 2021). eATP's upregulation of defence-related and wound-response genes *MPK3*, *WRKY40*, *CPK28* and *MC7* is P2K1/DORN1-dependent (Choi *et al*., 2014; Jewell *et al*., 2019) and was significantly impaired here in *cngc2-3* (Fig.4). *MC7* expression can be upregulated by the necrotrophic fungus *Alternaria brassicicola* (Kwon and Huang, 2013). Its CNGC2-dependent upregulation by eATP may relate specifically to DAMP signalling following ATP release by damaged cells. Wounded root cells not only release ATP (Dark *et al*., 2011) that could act as a DAMP for their neighbours but also release another DAMP, the peptide Pep1 (Hander *et al*., 2019). This is perceived in neighbouring cells by the cognate PM receptors PEPR1 and PEPR2 that relay to CNGC2 to cause $[Ca^{2+}]_{cyt}$ elevation (Qi *et al*., 2010). *PEPR2* is co-expressed with *P2K1/DORN1* (Tripathi *et al*., 2017). eATP also upregulates *PEPR1* and *PEPR2* transcription (Jewell *et al*., 2019) so CNGC2 could be a common component in these DAMP pathways to facilitate the adaptive response.

Acknowledgements

This work was funded by: UKRI BBSRC (BB/J014540/1); the framework of the 3rd call of the ERA-NET for Coordinating Action in Plant Sciences, with funding from the BBSRC (BB/S004637/1), US National Science Foundation (grant 1826803), and the ANR; University of Cambridge Commonwealth, European and International Trust; Jiangsu Normal University; a Discovery grant from the National Science and Engineering Research Council to KY. We thank Ms. S. Chakraborty and Mr. A. Sharif for technical assistance and Prof. G. Berkowitz for *dnd1*.

Author Contribution

Project conception: JS, BM, NL-F, VL, GS, JMD. Experimental design, execution and analyses: LW, YN, JS, REM, EM, KAW, AD, A-AV, LR, KY, WM, JMD. All authors contributed to writing.

Data Availability

All lines and data will be made available in a timely manner upon request.

References

Al-Younis I, Moosa B, Kwiatkowski M, Jaworski K, Wong A, Gehring C. 2021. Functional crypto-adenylate cyclases operate in complex plant proteins. *Frontiers in Plant Science*, **12**: 711749.

Chakraborty S, Toyota M, Moeder W, Chin K, Fortuna A, Champigny M, Vanneste S, Gilroy S, Beeckman T, Nambara E. 2021. Cyclic Nucleotide-Gated Ion Channel 2 modulates auxin homeostasis and signaling. *Plant Physiology* **187**(3): 1690-1703.

Chin K, DeFalco TA, Moeder W, Yoshioka K. 2013. The *Arabidopsis* cyclic nucleotide-gated ion channels AtCNGC2 and AtCNGC4 work in the same signaling pathway to regulate pathogen defense and floral transition. *Plant Physiology* **163**(2): 611-624.

Choi J, Tanaka K, Cao Y, Qi Y, Qiu J, Liang Y, Lee SY, Stacey G. 2014. Identification of a plant receptor for extracellular ATP. *Science* **343**(6168): 290-294.

Dark A, Demidchik V, Richards SL, Shabala S, Davies JM. 2011. Release of extracellular purines from plant roots and effect on ion fluxes. *Plant Signaling and Behavior* **6**(11): 1855-1857.

Demidchik V, Bowen HC, Maathuis FJM, Shabala SN, Tester MA, White PJ, Davies, JM. 2002. *Arabidopsis thaliana* root non-selective cation channels mediate calcium uptake and are involved in growth. *Plant Journal* **32**: 799-808.

Demidchik V, Nichols C, Dark A, Oliynyk M, Glover BJ, Davies JM. 2003. Is ATP a signaling agent in plants? *Plant Physiology* **133**: 456-461.

Demidchik V, Shang Z, Shin R, Thompson E, Rubio L, Laohavisit A, Mortimer JC, Chivasa S, Slabas AR, Glover BJ. 2009. Plant extracellular ATP signalling by plasma membrane NADPH oxidase and Ca^{2+} channels. *The Plant Journal* **58**(6): 903-913.

Dindas J, Scherzer S, Roelfsema MRG, von Meyer K, Müller HM, Al-Rasheid K, Palme K, Dietrich P, Becker D, Bennett MJ. 2018. AUX1-mediated root hair auxin influx governs SCF TIR1/AFB-type Ca^{2+} signaling. *Nature Communications* **9**(1): 1-10.

Dinneny JR, Long TA, Wang JY, Jung JW, Mace D, Pointer S, Barron C, Brady SM, Schiefelbein J, Benfey PN. 2008. Cell identity mediates the response of *Arabidopsis* roots to abiotic stress. *Science* **320**(5878): 942-945.

Jaffe M. 1973. The role of ATP in mechanically stimulated rapid closure of the Venus's flytrap. *Plant Physiology* **51**(1): 17-18.

Jarratt-Barnham E, Wang L, Ning Y, Davies JM. 2021. The complex story of plant cyclic nucleotide-gated channels. *International Journal of Molecular Sciences* **22**(2): 874.

Jewell JB, Sowders JM, He R, Willis MA, Gang DR, Tanaka K. 2019. Extracellular ATP shapes a defense-related transcriptome both independently and along with other defense signaling pathways. *Plant Physiology* **179**(3): 1144-1158.

Knight H, Trewavas AJ, Knight MR 1997. Recombinant aequorin methods for measurement of intracellular calcium in plants. *Plant Molecular Biology Manual*: Springer, Dordrecht, Netherlands1-22. Eds. S.B. Gelvin, R.A. Schilperoort.

Krogman W, Sparks JA, Blancaflor EB 2020. Cell type-specific imaging of calcium signaling in *Arabidopsis thaliana* seedling roots using GCaMP3. *International Journal of Molecular Sciences* **21**: 6385-6399.

Kumar S, Tripathi D, Okubara PA, Tanaka K. 2020. Purinoceptor P2K1/DORN1 enhances plant resistance against a soilborne fungal pathogen, *Rhizoctonia solani*. *Frontiers in Plant Science* **11**: 1479.

Kwon SI, Hwang DJ. 2013. Expression analysis of the metacaspase gene family in *Arabidopsis*. *Journal of Plant Biology* **56**(6): 391-398.

Lew RR, Dearnaley JD. 2000. Extracellular nucleotide effects on the electrical properties of growing *Arabidopsis thaliana* root hairs. *Plant Science* **153**(1): 1-6.

Matthus E, Sun J, Wang L, Bhat MG, Mohammad-Sidik AB, Wilkins KA, Leblanc-Fournier N, Legué V, Moulia B, Stacey G. 2019a. DORN1/P2K1 and purino-calcium signalling in plants: making waves with extracellular ATP. *Annals of Botany* **124**(7): 1227-1242.

Matthus E, Wilkins KA, Swarbreck SM, Doddrell NH, Doccula FG, Costa A, Davies JM. 2019b. Phosphate starvation alters abiotic-stress-induced cytosolic free calcium increases in roots. *Plant Physiology* **179**(4): 1754-1767.

Mohammad-Sidik A, Sun J, Shin R, Song Z, Ning Y, Matthus E, Wilkins KA, Davies JM. 2021. *Annexin 1* is a component of eATP-induced cytosolic calcium elevation in *Arabidopsis thaliana* roots. *International Journal of Molecular Sciences* **22**(2): 494.

Pham AQ, Cho S-H, Nguyen CT, Stacey G. 2020. *Arabidopsis* lectin receptor kinase P2K2 is a second plant receptor for extracellular ATP and contributes to innate immunity. *Plant Physiology* **183**(3): 1364-1375.

Qi Z, Verma R, Gehring C, Yamaguchi Y, Zhao Y, Ryan CA, Berkowitz GA. 2010. Ca^{2+} signaling by plant *Arabidopsis thaliana* Pep peptides depends on AtPepR1, a receptor with guanylyl cyclase activity, and cGMP-activated Ca^{2+} channels. *Proceedings of the National Academy of Sciences USA* **107**(49): 21193-21198.

Rincón-Zachary M, Teaster ND, Sparks JA, Valster AH, Motes CM, Blancaflor EB. 2010. Fluorescence resonance energy transfer-sensitized emission of yellow cameleon 3.60 reveals root zone-specific calcium signatures in *Arabidopsis* in response to aluminum and other trivalent cations. *Plant Physiology* **152**(3): 1442-1458.

Tanaka K, Swanson SJ, Gilroy S, Stacey G. 2010. Extracellular nucleotides elicit cytosolic free calcium oscillations in *Arabidopsis*. *Plant Physiology* 154: 705–719.

Tian W, Hou C, Ren Z, Wang C, Zhao F, Dahlbeck D, Hu S, Zhang L, Niu Q, Li L, Staskowicz BJ, Luan S. 2019. A calmodulin-gated calcium channel links pathogen patterns to plant immunity. *Nature* **572**(7767): 131-135.

Tripathi D, Zhang T, Koo AJ, Stacey G, Tanaka K. 2017. Extracellular ATP acts on jasmonate signaling to reinforce plant defense. *Plant Physiology* **176**: 511-523.

Waadt R, Köster P, Andrés Z, Waadt C, Bradamante G, Lampou K, Kudla J, Schumacher K. 2020. Dual-reporting transcriptionally linked genetically encoded fluorescent indicators resolve the spatiotemporal coordination of cytosolic abscisic acid and second messenger dynamics in *Arabidopsis*. *Plant Cell* **32**(8): 2582-2601.

Wang Y-F, Munemasa S, Nishimura N, Ren H-M, Robert N, Han M, Puzõrjova I, Kollist H, Lee S, Mori I. 2013. Identification of cyclic GMP-activated nonselective Ca^{2+}-permeable cation channels and associated CNGC5 and CNGC6 genes in *Arabidopsis* guard cells. *Plant Physiology* **163**(2): 578-590.

Wang L, Wikins K, Davies J. 2018. *Arabidopsis* DORN1 extracellular ATP receptor; activation of plasma membrane K^+-and Ca^{2+}-permeable conductances. *New Phytologist* **218**: 1301-1304.

Wang L, Stacey G, Leblanc-Fournier N, Legué V, Moulia B, Davies JM. 2019. Early extracellular ATP signaling in *Arabidopsis* root epidermis: A multi-conductance process. *Frontiers in Plant Science* **10**: 1064.

Wu Y, Yin H, Liu X, Xu J, Qin B, Feng K, Kang E, Sahng Z. 2021. P2K1 receptor, heterotrimeric Gα protein and CNGC2/4 are involved in extracellular ATP-promoted ion influx in the pollen of *Arabidopsis thaliana*. *Plants* **10**:1743.

Zhu R, Dong X, Hao W, Gao W, Zhang W, Xia S, Liu T, Shang Z. 2017. Heterotrimeric G protein-regulated Ca^{2+} influx and PIN2 asymmetric distribution are involved in *Arabidopsis thaliana* roots' avoidance response to extracellular ATP. *Frontiers in Plant Science* **8**: 1522.

Figure legends

Fig. 1. CNGC2 is required for eATP-induced depolarisation of primary root elongation zone epidermal plasma membrane (PM) potential (E_m). (a) A representative example of an *Arabidopsis* Col-0 root indicating the elongation zone where a single epidermal or cortical cell was impaled with a microelectrode (represented by the blue triangle). Bar = 0.1 cm. (b) Representative epidermal E_m recordings from Col-0, *cngc2-3* and *cngc2-3,CNGC2::CNGC2* treated with 300 µM eATP (black triangles indicate addition). (c) Mean ± SE time courses of the response to 300 µM eATP for Col-0 (n = 9), *cngc2-3* (n = 9) and *cngc2-3,CNGC2::CNGC2* (n = 5). The chemical addition time was set to 0 on the x axis. (d) Comparison of mean ± SE E_m before eATP (-ATP) and after eATP treatment (+ATP; maximum depolarisation). Different lower-case letters on the top of vertical bars indicate significant difference between means ($p < 0.05$). (e) Col-0 and *cngc2-3, CNGC2::CNGC2* took similar times for E_m to recover from depolarisation. (f) *cngc2-3, CNGC2::CNGC2* E_m depolarised more rapidly than Col-0 in response to eATP. (g) Representative epidermal E_m recordings from Col-0. Top trace, response to 300 µM $MgSO_4$ (n = 8); second trace, response to 300 µM Na_2SO_4 (n = 6); third trace, response to 300 µM eATP in the presence of 5 mM EGTA (n = 5); bottom trace, response to 300 µM eATP in the presence of 0.5 mM $LaCl_3$ (n = 3). Mean time courses are in Fig. S1. (h) Comparison of mean ± SE E_m before and after addition of 300 µM $MgSO_4$ or Na_2SO_4 to Bath Solution (BS) and before and after addition of eATP in the presence of 5 mM EGTA or 0.5 mM $LaCl_3$ in the BS. BS contained (in mM) 2 $CaCl_2$, 0.1 KCl, 1 MES/Tris (pH 6.0). *, $p < 0.05$; n.s, not significant.

Fig. 2. eATP activates inward currents in *Arabidopsis* Col-0 but not *cngc2-3* root elongation zone epidermal protoplasts. (a). Left panel: Typical whole-cell PM currents in Col-0 protoplasts before (-; black) and after (+; light blue) application of 300 µM eATP. eATP effects were observed 30 s to 3 minutes after addition. Bath solution contained (mM): 50 $CaCl_2$, 1 KCl, 10 MES-Tris (pH 5.6). Pipette solution comprised (mM): 5 $BaCl_2$, 20 KCl, 10 HEPES-Tris (pH 7.5). Centre panel: Mean ± SE current-voltage (*I-V*) relationships of Col-0 before (-), after (+) ATP and in 100 µM Gd^{3+} (dark blue; the calcium channel blocker was applied after eATP treatment) (n = 4). Right panel: Comparison of the inward currents at -190 mV (solid bars) and the outward currents at +50 mV (hollow bars) before and after eATP addition and in the presence of Gd^{3+}. Gd^{3+} block of control inward currents is also evident. (b) As (a) but for *cngc2-3* protoplasts. The mutant did not respond to eATP even with an extended observation period (10 min). Data are means ± SE (n = 4; *, $p < 0.05$; n.s, not significant).

Fig. 3. CNGC2 contributes to the eATP-induced $[Ca^{2+}]_{cyt}$ increase in *Arabidopsis* roots. (a) Mean ± SE $[Ca^{2+}]_{cyt}$ time-course in control experiments (n = 18-19 roots in 3 independent trials). NaCl was applied at 35 s to individual excised roots of Col-0 or *dnd1* (black inverted triangle; 0.6 mM final concentration). Assay solution contained 2 mM Ca^{2+} to match E_m recordings. (b) Left panel: Amplitude of touch-induced peak $[Ca^{2+}]_{cyt}$ increase after baseline-subtraction. The *dnd1* response was not normally distributed and the Mann-Whitney test was used in significance testing. Right panel: Area under the curve (AUC) after baseline-subtraction was analysed as an estimate of total $[Ca^{2+}]_{cyt}$ mobilised (Matthus *et al*., 2019b). (c) Mean ± SE $[Ca^{2+}]_{cyt}$ time-course with 300 µM eATP applied at 35s (n = 38 for both Col-0 and *dnd1* in 3 independent trials). Dotted lines indicate time of peak response of Col-0. (d) *dnd1* had a significantly smaller $[Ca^{2+}]_{cyt}$ response when compared to Col-0, but not in the touch-peak. The *dnd1* response for the touch peak was not normally distributed and the Mann-Whitney test was used in significance testing. Peaks were compared with Col-0 at the equivalent time-point. Each dot in box plots represents an individual recording. The middle line and the triangle in the box plot are the median and mean, respectively. The box outline (hinges) denote median of the upper and the lower half of the data. The bars denote entirety of data excluding outliers; outliers are depicted by individual points outside the boxplot bars. ***, $p < 0.001$; *, $p < 0.05$; n.s, not significant.

Fig. 4. CNGC2 is implicated in the eATP-induced transcriptional response in *Arabidopsis* roots. Col-0, *cngc2-3* and *cngc2-3,CNGC2::CNGC2* whole roots were treated with control (NaCl) buffer

(Mock) or 300 µM eATP for 5 minutes (ATP-5) or 30 minutes (ATP-30). Two housekeeping genes, *AtUBQ*10 and *AtTUB4*, were used for data normalization. Data are mean ± SE from three independent trials with $n > 4$ biological replicates. (a) Results for *MPK3*. (b) Results for *WRKY40*. (c) Results for *CPK28*. (d) Results for *MC7*. Significant differences between *cngc2-3* and the other two genotypes were found at ATP-30 and p values are shown. No significant differences were observed between Col-0 and *cngc2-3,CNGC2::CNGC2* at ATP-30. Asterisks indicate the statistical significance relative to the mock treatment (*, $p < 0.05$; **, $p < 0.01$; ***, $p < 0.001$). (e) Summary of possible signalling events at epidermis and cortex. DORN1/P2K1 and P2K2 (P2) together promote CNGC2 channel opening to mediate Ca^{2+} influx, E_m depolarization and $[Ca^{2+}]_{cyt}$ increase. The mechanism is unknown but could include phosphorylation or direct production of cyclic nucleotide monophosphates by cryptic catalytic centres (Al-Younis *et al*., 2021). eATP could follow the apoplastic pathway to initiate events in cortical cells, potentially through the P2 receptor complex and with CNGC4 as a component of Ca^{2+} influx, E_m depolarization and $[Ca^{2+}]_{cyt}$ increase. Other stimuli could be transmitted from the epidermis to the cortex in a CNGC2-independent pathway.

Supporting Information

Methods S1 Genotyping *cngc* insertional and complemented mutants.

Table S1 Primers used for genotyping T-DNA mutant lines and qRT-PCR.

Methods S2 Growth conditions.

Methods S3 Membrane voltage measurement.

Methods S4 Patch clamp recordings.

Methods S5 qRT-PCR analysis of gene expression.

Table S2 Mean ± SE membrane voltage (E_m) measurements.

Fig. S1 Controls for depolarisation of elongation zone epidermis and effect of extracellular Ca^{2+} chelation or channel block.

Fig. S2 Growth of *cngc2-3* and receptor expression.

Fig. S3 eATP did not depolarise *dnd1* elongation zone epidermis.

Fig. S4 Single receptor mutants supported a small but significant eATP-induced depolarisation of elongation zone epidermal E_m.

Fig. S5 The *p2k1p2k2* double receptor mutant lacked the eATP-induced depolarisation of elongation zone epidermal E_m.

Fig. S6 *cngc4-5* supported a significant eATP-induced depolarisation of elongation zone epidermal E_m.

Fig. S7 eATP did not activate inward currents in *dorn1-3* root elongation zone epidermal protoplasts.

Fig. S8 CNGC2 contributed to the eATP-induced $[Ca^{2+}]_{cyt}$ increase in roots.

Fig. S9 CNGC2 is not required for eATP-induced depolarisation of primary root elongation zone cortical plasma membrane potential but CNGC4 is involved.

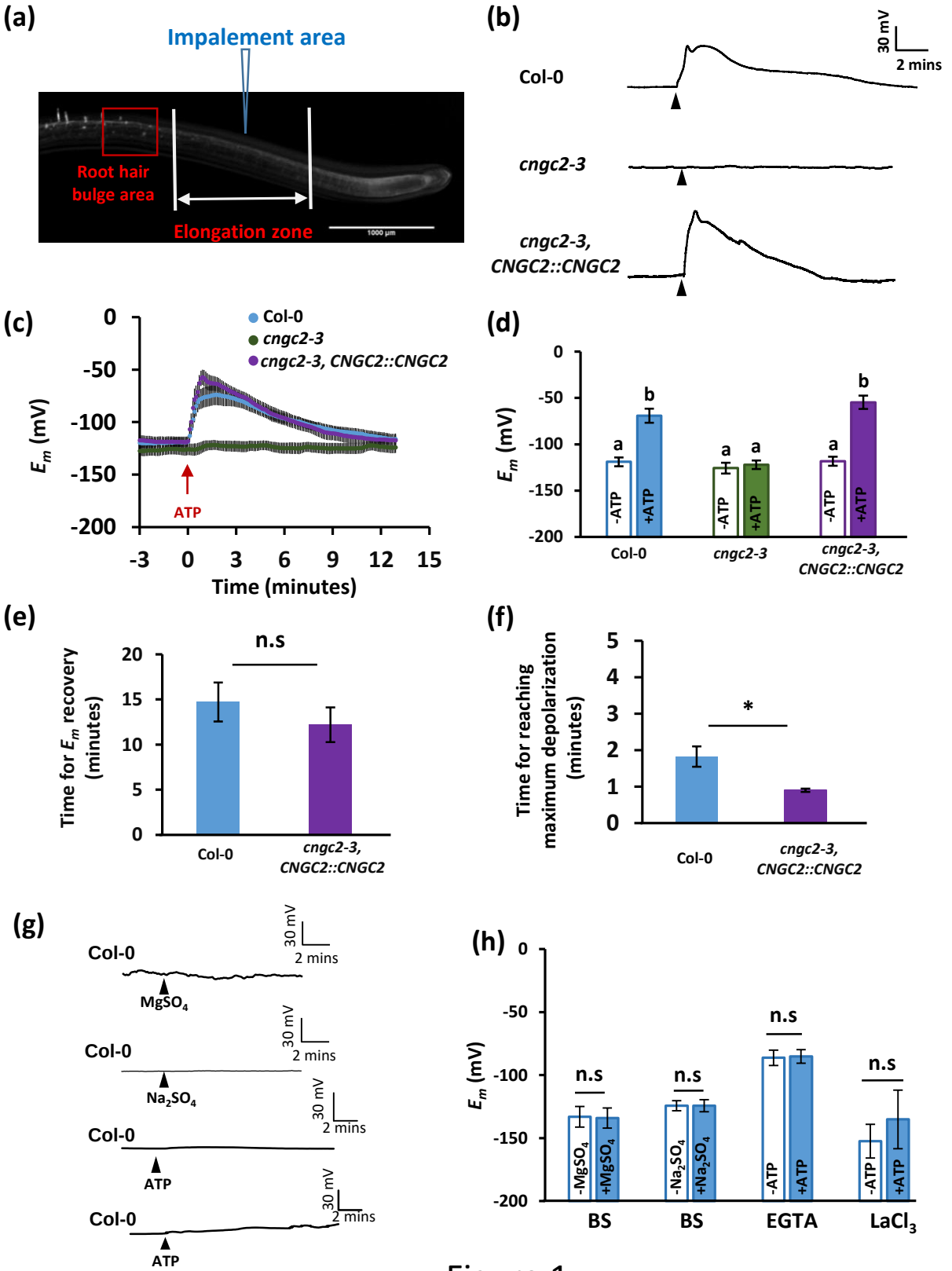
(a)
Impalement area
Root hair bulge area
Elongation zone
1000 µm
(b)
30 mV
2 mins
Col-0
cngc2-3
cngc2-3, CNGC2::CNGC2
(c)
Col-0
cngc2-3
cngc2-3, CNGC2::CNGC2
E_m (mV)
ATP
Time (minutes)
(d)
E_m (mV)
a
b
-ATP
+ATP
Col-0
cngc2-3
cngc2-3, CNGC2::CNGC2
(e)
n.s
Time for E_m recovery (minutes)
Col-0
cngc2-3, CNGC2::CNGC2
(f)
*
Time for reaching maximum depolarization (minutes)
Col-0
cngc2-3, CNGC2::CNGC2
(g)
Col-0
$MgSO_4$
Na_2SO_4
ATP
30 mV
2 mins
(h)
E_m (mV)
n.s
-$MgSO_4$
+$MgSO_4$
-Na_2SO_4
+Na_2SO_4
-ATP
+ATP
BS
BS
EGTA
$LaCl_3$

Figure 1

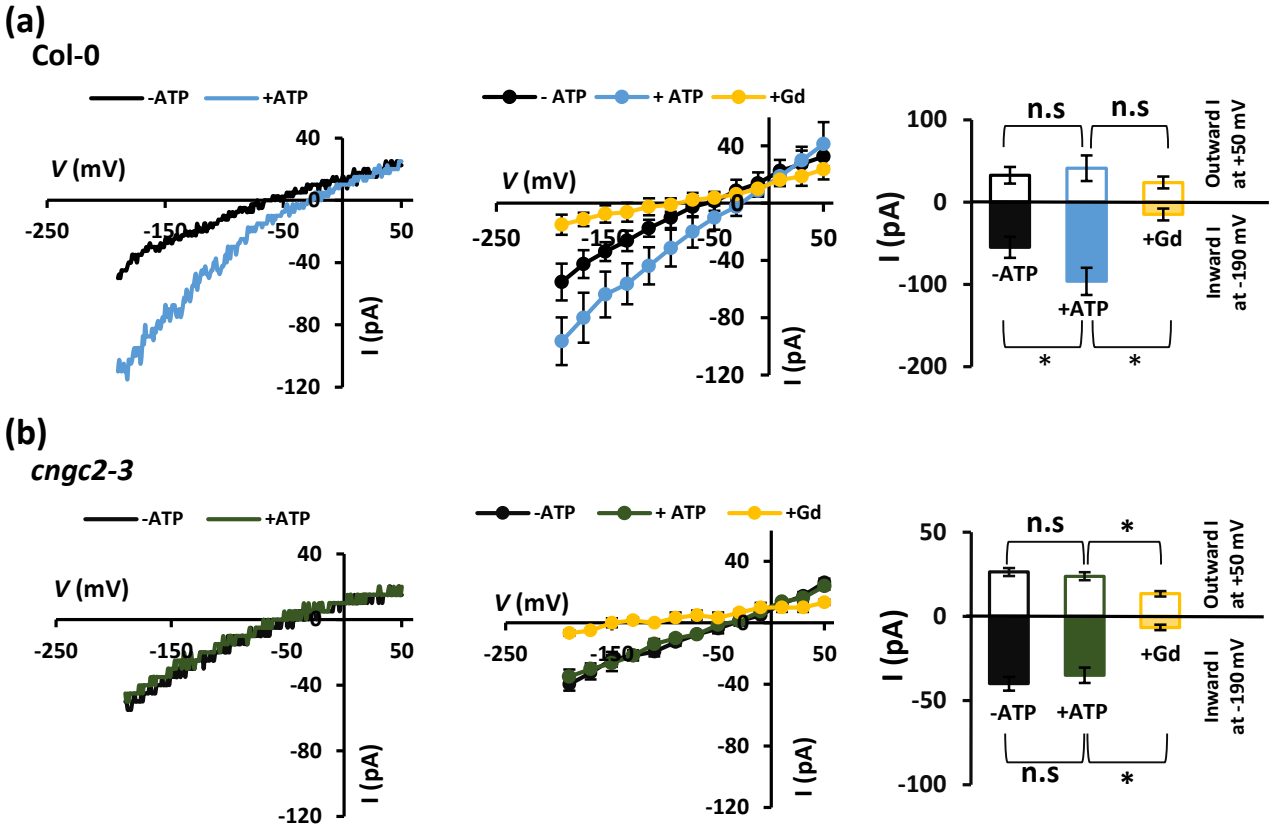
(a)
Col-0
-ATP
+ATP
V (mV)
I (pA)
+Gd
n.s
Outward I at +50 mV
Inward I at -190 mV
(b)
cngc2-3

Figure 2

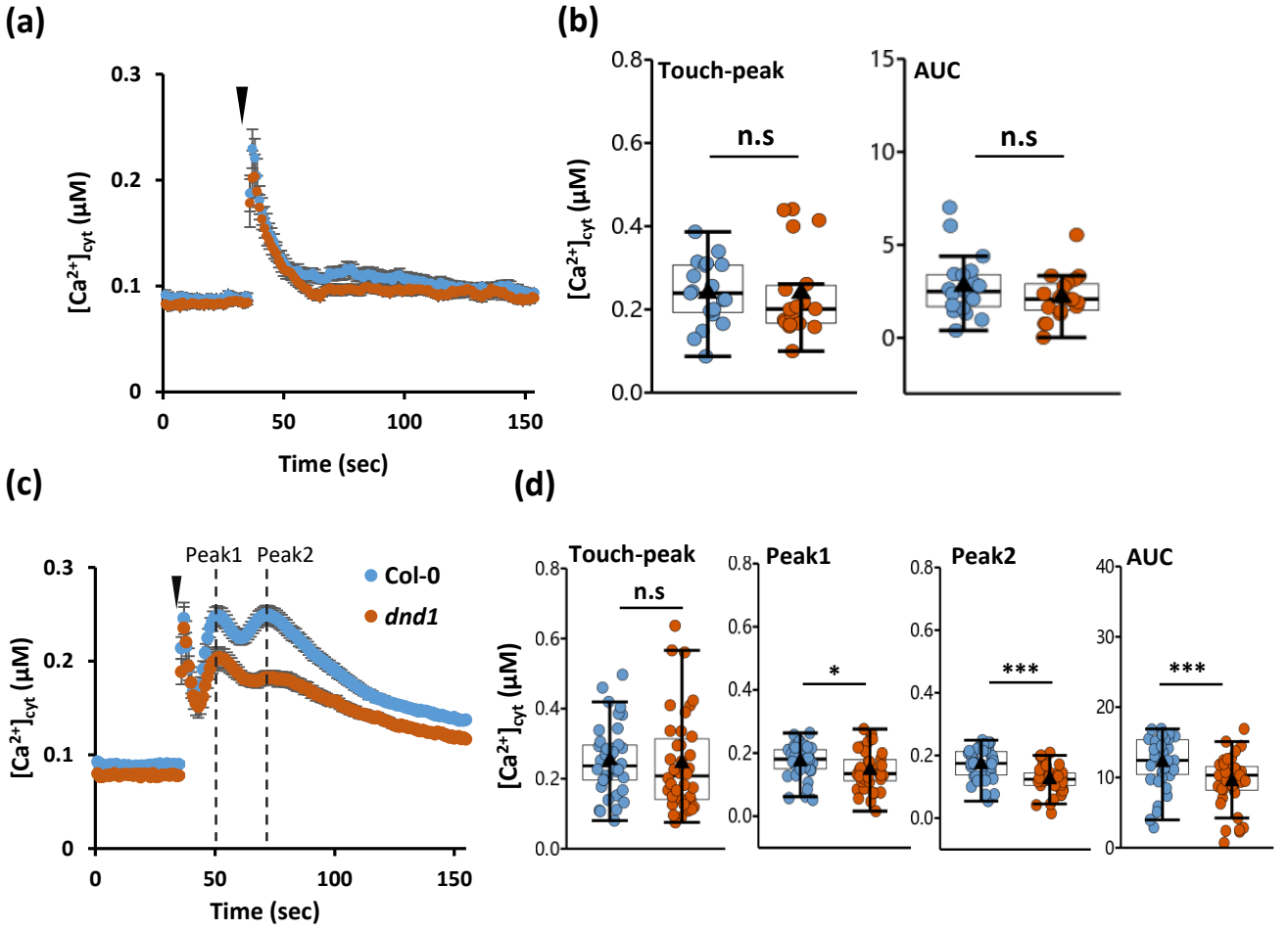
(a)
(b)
(c)
(d)
[Ca2+]cyt (μM)
Time (sec)
Touch-peak
AUC
n.s
Peak1
Peak2
Col-0
dnd1
*
***

Figure 3

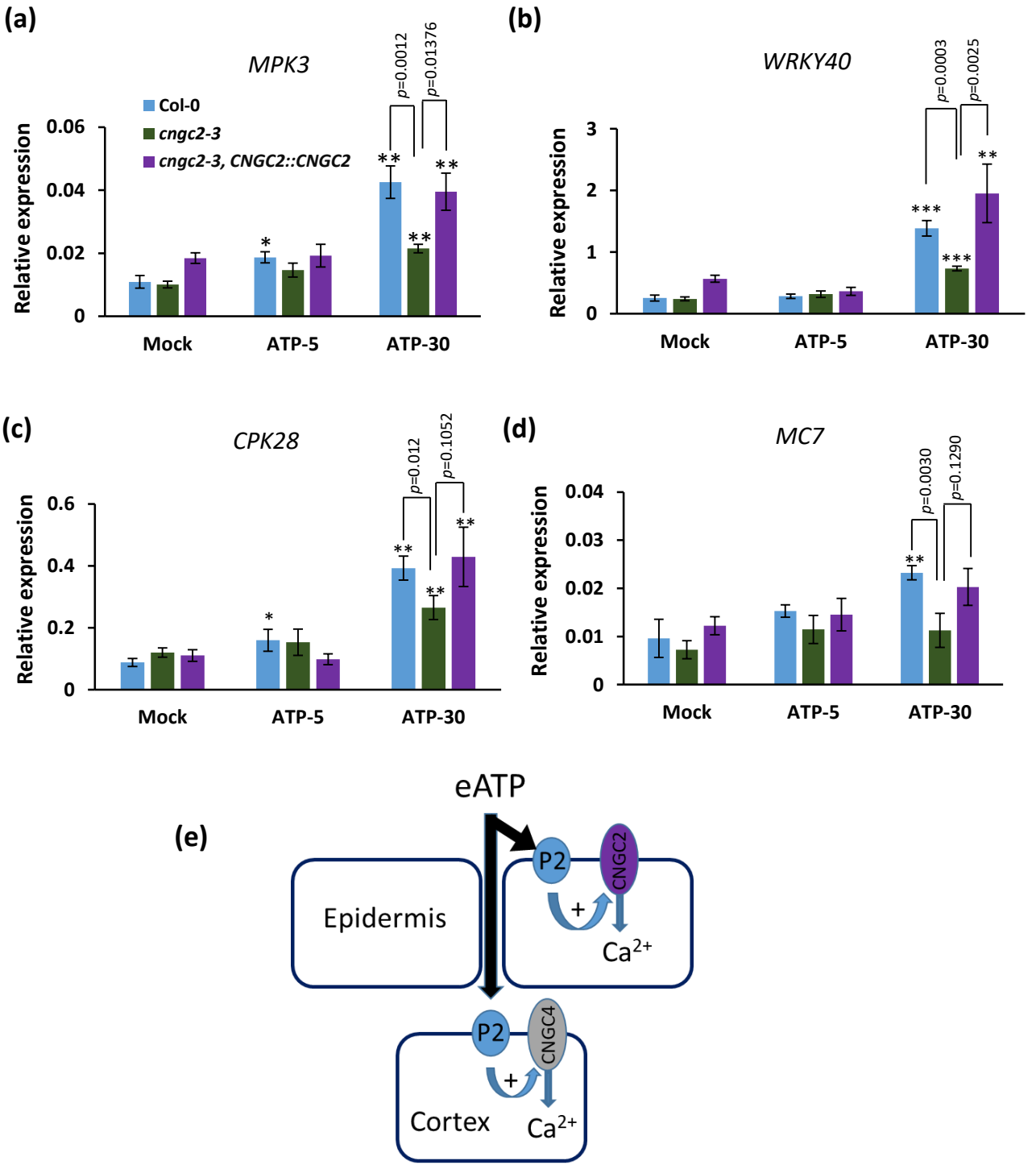
(a)
MPK3
Col-0
cngc2-3
cngc2-3, CNGC2::CNGC2
Relative expression
0.06
0.04
0.02
0
p=0.0012
p=0.01376
Mock
ATP-5
ATP-30
(b)
WRKY40
Relative expression
3
2
1
0
p=0.0003
p=0.0025
Mock
ATP-5
ATP-30
(c)
CPK28
Relative expression
0.6
0.4
0.2
0
p=0.012
p=0.1052
Mock
ATP-5
ATP-30
(d)
MC7
Relative expression
0.04
0.03
0.02
0.01
0
p=0.0030
p=0.1290
Mock
ATP-5
ATP-30
(e)
eATP
Epidermis
P2
CNGC2
+
Ca2+
P2
CNGC4
+
Cortex
Ca2+

Figure 4